NEURAL NETWORK BASED PROCESSING OF THERMAL NDE DATA FOR CORROSION DETECTION

D. R. Prabhu
Analytical Services & Materials, Inc.
MS 231, NASA Langley Research Center
Hampton, VA 23681

W. P. Winfree
Nondestructive Evaluation Sciences Branch
MS 231, NASA Langley Research Center
Hampton, VA 23681

INTRODUCTION

Subsurface corrosion in aircraft structure is a major concern in lap joints and other joints. Small open gaps in the joints form regions where moisture can be trapped. The trapped water often produces a chemical environment in the regions which accelerates the corrosion process. Corrosion considerably reduces structural strength and load-bearing capacity of the structure. To ensure flight safety, it is imperative to detect subsurface corrosion as early as possible during aircraft maintenance operations. Since long down-times of commercial aircraft translate to large operating costs for airline industries, it is desirable to develop techniques that can consistently and reliably detect corrosion by rapidly scanning the aircraft. Towards this goal, the thermal technique, which is a nondestructive, noncontacting technique capable of rapidly inspecting aircraft structures for defects such as disbonds, corrosion, and cracks is currently under development [1]. Also under parallel development are techniques such as ultrasonics, magneto-optics, shearography, electromagnetics, and radiography.

The effectiveness of a particular NDE technique depends not only on the instrumentation, but also on techniques that are used in conjunction with the inspection to efficiently and accurately extract relevant information from the acquired data [2]. Several processing techniques have been developed for use in conjunction with thermal imaging to clearly reveal the flaws and to provide quantitative information concerning the state of the test region. One such technique employs neural networks which have recently shown considerable success in a variety of applications. Neural networks were recently used to detect disbonds in lap joints and doubler joints through processing thermal data [3]. High classification accuracies were achieved and the resulting network output image was easily thresholded to yield a binary image clearly showing the extent of bond in the test region. In

Review of Progress in Quantitative Nondestructive Evaluation, Vol. 12
Edited by D.O. Thompson and D.E. Chimenti, Plenum Press, New York, 1993

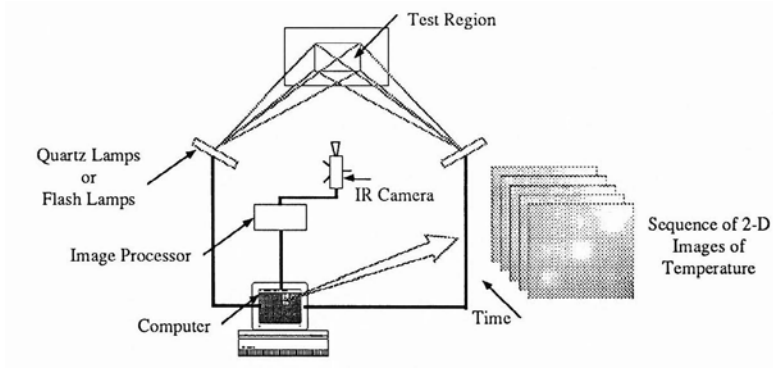

Figure 1. Schematic of the thermal NDE test setup.

this paper, a novel technique is presented that uses two neural networks which work together to process thermal NDE data for both corrosion detection and estimation.

THERMAL NDE TEST SETUP

The thermal NDE test setup consists of two sets of quartz lamps or flash lamps that provide a heat influx to the test region. An IR camera connected to a real-time image processor scans and digitizes the temperature across the test region up to 30 times per second. The image processor is connected to a microcomputer which also controls the heat lamps. A schematic of the test setup is shown in Fig. 1.

Thermal data acquired from the test region is in the form of a time sequence of 2-D temperature image frames, with each frame obtained by averaging a number of images of temperatures in time to increase the signal to noise ratio. The heat-up time and the number of averages per frame depend on the heating protocol used for the experiment, which in turn is chosen based on the geometry and material properties of the test sample to yield good contrast in the resulting thermal data.

SAMPLE GEOMETRY AND THERMAL DATA

Two samples with fabricated material loss defects were used in this study. Sample 1 consisted of two layers of aluminum (7075-T6) with dimensions 381 mm X 381 mm X 3.175 mm. Material was removed on the inner surface of the outer layer of aluminum to simulate subsurface corrosion in aircraft lap joints of various amounts and sizes as shown in Fig. 2a. No by-products of corrosion were substituted in place of air in the material loss volumes. There were 9 defects with material losses of 25%, 50%, and 75% in three different sizes, namely, squares of sides 25.4 mm (1 in), 50.8 mm (2 in), and 76.2 mm (3 in). Sample 2 was an aluminum (2024-T3) plate with dimensions 280 mm X 190 mm X 1 mm. Simulated corrosion defects with 5%, 10%, and 15% material loss were fabricated in the sample by milling out material on the non-imaging side, as shown in Fig. 2b.

Sample 1 was thermographically tested using quartz lamps heating. The sample was imaged with heat influx for approximately 8 seconds, following which the heat influx was turned off and the sample was imaged for post-heating response for approximately another 8 seconds. The temperature vs. time curves corresponding to central locations of all 9 defects is presented in Fig. 3. It can be seen in the plot that the thermal curves correspond-

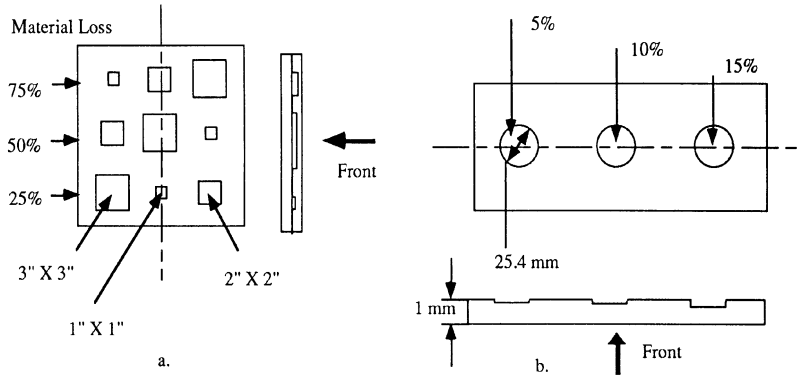

Figure 2. Geometry of corrosion (material loss) samples -- a. Sample 1 (7075-T6 Al) with material losses of 25%, 50%, and 75% of outer aluminum layer, and b. Sample 2 (2024 Al) with smaller material losses of 5%, 10%, and 15%.

ing to 75%, 50%, and 25% material loss are reasonably separated in the first few frames due to different heating rates. Unfortunately, it is difficult to classify the 25% material loss locations from good locations in these frames. At a later time, due to lateral heat diffusion, the curve corresponding to the smallest 75%-loss location drops below that corresponding to the largest 50%-loss location. A similar phenomenon can be seen for the smallest 50%-loss location and the largest 25%-loss location. After approximately 5 secs, it is not possible to obtain threshold values for temperature that can correctly separate regions of various amounts of material loss. Even though the curves corresponding to good locations and the 25%-loss locations show slight temperature differences, it is not possible to find a single threshold value for any given frame which accurately separates the smallest 25%-loss locations. These features of the temperature vs. time curves can be seen in the contrast-enhanced temperature images presented in Fig. 4. for a subset of the available frames.

Consequently, a data processing technique that uses all the information in the curves is desirable to achieve a high classification accuracy for corrosion estimation. In this paper, a novel method using two neural networks - a flaw detector network and a corrosion estima-

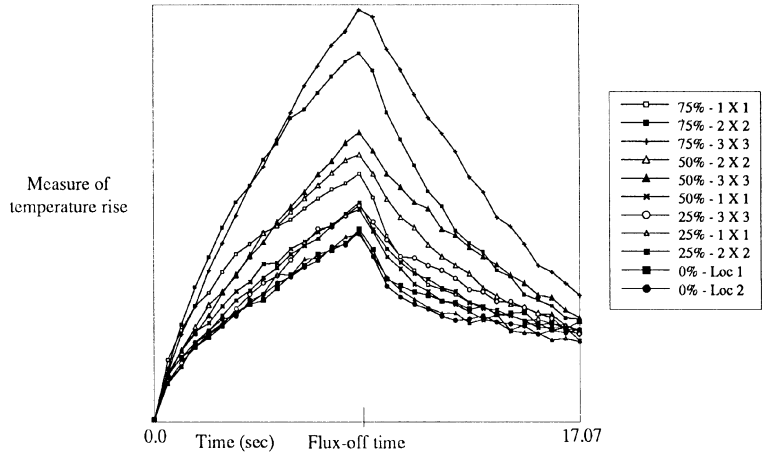

Figure 3. Temperature vs. time curves for quartz lamp heating of sample 1 for various material loss locations. Heat-up time = 8.53s, time corresponding to last frame = 17.07s.

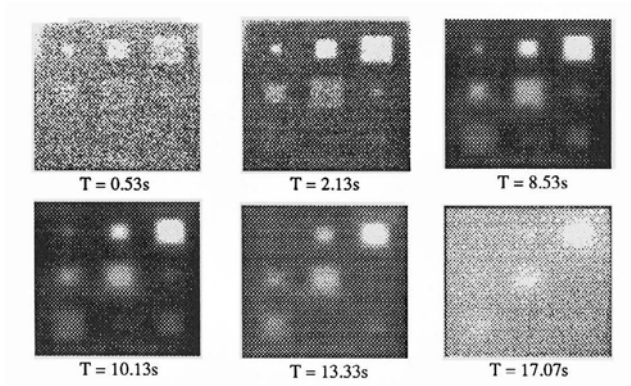

Figure 4. Contrast enhanced temperature images of sample 1 at various times.

tor network - is presented that yields both high classification and corrosion estimation accuracies. The technique will be illustrated using thermal data for sample 1, and will be subsequently used to process thermal data for sample 2.

APPLICATION OF NEURAL NETWORKS

Neural networks or multilayered perceptrons consist of a set of highly interconnected nonlinear processing elements that operate in parallel. Each interconnection between neuron has an associated connection weight that can be adjusted to achieve desired network behavior through a training process. Several different network architectures and training algorithms are available, and the reader is referred to [4] for details. In this paper, 3-layered and 4-layered networks will be used with backpropagation training.

By using the entire temperature vs. time curve as the input to the network and through suitable training, the network can be made to respond in a desirable way to various features of the thermal curves. In [3], similar temperature vs. time curves have been classified as corresponding to bonded and disbonded location of aircraft adhesive joints using a 3-layered network with a single output neuron. A neuron state of "off" indicates a good, bonded location, and that of "on" indicates a disbonded location. Such a network with a single output neuron, as shown in Fig. 5a, solving a two-class flaw/no-flaw classification problem will be referred to as a "flaw detector network" in this paper. A neural network can also be trained to process thermal data to yield the amount of corrosion or material loss. An estimation problem of such a kind can be transformed to a classification problem through a binning process, with each bin corresponding to a certain range of material loss. The corresponding network that classifies thermal curves into various bins will be referred to as a "corrosion estimator network" in this paper. A sample estimator network with 10 bins is presented in Fig. 5b. The network is trained such that one and only one output neuron activates for any given thermal curve.

Results obtained for sample 1 using a 32 X 30 X 1 flaw detector network trained using 99 input-output patterns is presented in Fig. 6a which clearly shows the 9 defects of different amounts of material loss. One of the advantages of using neural networks for NDE is the ability to easily threshold neuron output values to obtain a binary image clearly showing the flaws in the test region. Since a neuron state of "off" corresponds to an output value of 0.0, and that of "on" corresponds to 1.0 for a sigmoid neuron activation function, neuron

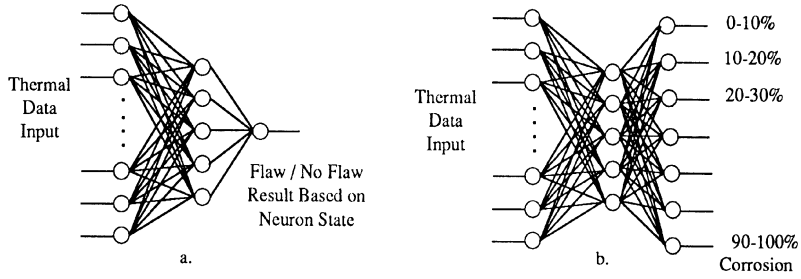

Figure 5. Flaw detector and corrosion estimator networks -- a. Flaw detector network with one output neuron, and b. Corrosion estimator network showing a binned output.

output is thresholded at a value of 0.5 to obtain a binary image. The thresholded binary image corresponding to the network output image of Fig. 6a is shown in Fig. 6b, with the white pixels representing flawed locations. The classification accuracy achieved is seen to be fairly high, with misclassifications restricted to the border regions between flawed and unflawed locations. Classification accuracy is defined as the percentage of locations correctly classified as flawed or unflawed. The results obtained using a 3-bin classification of the same thermal data for sample 1 obtained using a 32 X 24 X 12 X 3 estimator network are presented in Figs. 7a-c. Fig. 7a is an image of the output values of neuron 1, which is trained to yield an output value of 1.0 for thermal curves corresponding to 75% material loss, and an output value of 0.0 for all other cases. Similarly, neurons 2 and 3 are trained to respond to 50% and 25% material losses respectively. Figs. 7a and 7b show the 75% and 50% material loss flaws very clearly; however, Fig. 7c seems unacceptable due to the large percentage of unflawed regions that are classified into the 25% material loss bin. These results can be improved by increasing the number of training patterns and obtaining a network that exhibits the highest classification accuracy for the training set used. Typically, one needs a larger network to learn an augmented training set which clearly needs longer training periods. In what follows, results obtained using the two networks will be combined to yield high overall corrosion estimation accuracies.

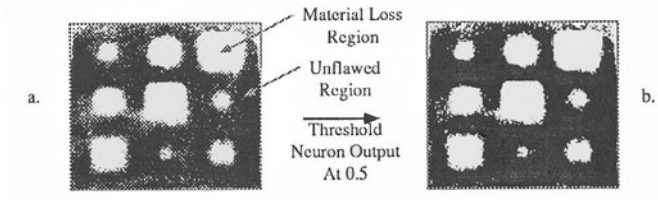

Figure 6. Flaw detector network output clearly showing flawed and flaw-free locations in sample 1-- a. Neural network output image, and b. Image thresholded at 0.5.

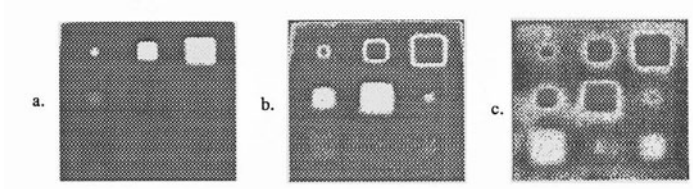

Figure 7. Binned output images of sample 1 using a corrosion estimator network - a. Output of neuron 1 (75%), b. Output of neuron 2 (50%), and c. Output of neuron 3 (25%).

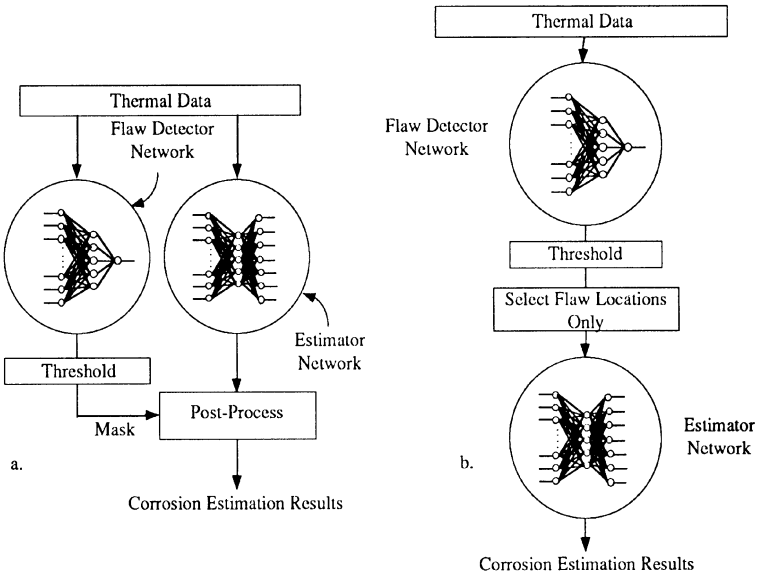

Figure 8. Two possible architectures for dual network processing -- a. Parallel architecture, and b. Serial architecture.

New Technique Using Detector And Estimator Networks

The key idea in this paper is to use both the flaw detector network and the estimator network to process the same thermal data so as to obtain an end effect that is greater than what can be achieved by using either of them processing the data separately. In Fig. 7c, a large percentage of unflawed locations are classified as 25% material loss locations. However, from the results obtained through flaw-detector processing, the misclassified locations are known to be good, unflawed locations. This leads to the first architecture for dual network processing - the parallel architecture, as shown in Fig. 8a. The thermal data to be processed is classified by both the flaw detector and the estimator networks. The results from the flaw detector network are thresholded at 0.5 to obtain a binary image clearly showing flawed and unflawed locations. This binary image is later used as a mask to post-process the results obtained using the estimator network. Post-processing involves thresholding each image corresponding to the output neurons of the estimator network, followed by logical AND operations between each thresholded image and the mask image. The image corresponding to the highest amount of material loss is processed first, and in a decreasing order the image corresponding to the smallest amount of material loss is processed last. Alternatively, the two networks can be used in a serial architecture as shown in Fig. 8b, where the thermal data is processed first by the flaw detector network. The resulting image is thresholded as before to obtain a binary image. From this image, only the flaw locations are picked out and their corresponding thermal curves are further processed using the estimator network. Thermal curves corresponding to unflawed locations are not processed any further. The final results obtained using the dual network processing described here will be presented in the following section.

Results From Dual Network Processing

The thresholded image of Fig. 6b was used as a mask to process results shown in Figs.

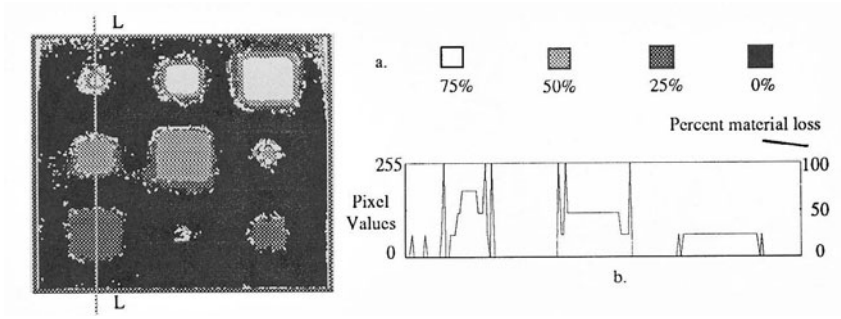

Figure 9. Results of dual network processing of thermal NDE data for sample 1-- a. Output image clearly showing percentages of corrosion, and b. Pixel value plot along line LL.

7a-c. The resulting image through dual network processing are presented in Fig. 9a. All the misclassifications in Fig. 7c are clearly masked out by the flaw/no-flaw image used as a mask. A plot of pixel values along line LL is given in Fig. 9b. The pixel values are chosen to be proportional to the amount of material loss during each logical AND operation. The resulting image is seen to accurately show the corroded state of sample 1. The temperature vs. time curves obtained through flash heating of sample 2 are presented in Fig. 10. The duration of the flash for the experiment was 0.01 sec. The thermal data consists of 16 frames, with 0.27 sec between successive frames. Since the material losses are relatively small, the curves are close to those corresponding to unflawed locations. Network output image obtained through a 5 X 2 X 1 flaw detector network using only 35 training patterns is shown in Fig. 11a. 5 data points between 0.53 sec and 1.6 sec (Frames 3 through 7) were

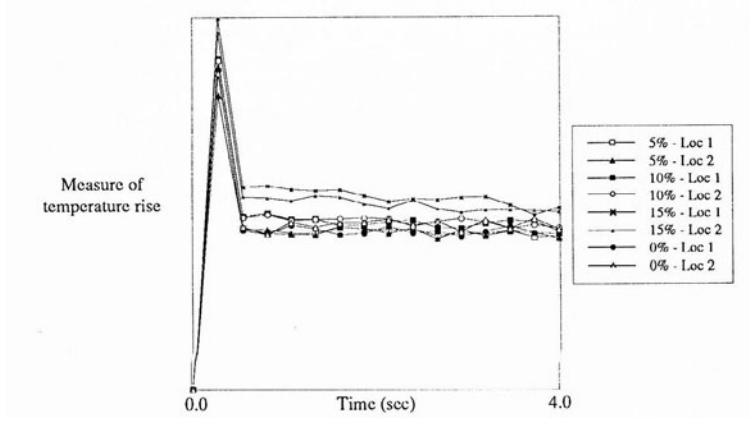

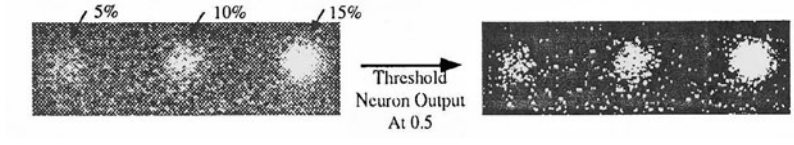

Figure 11. Results of processing thermal data for sample 2 using a flaw detector network -- a. Network output image, and b. Thresholded image at 0.5.

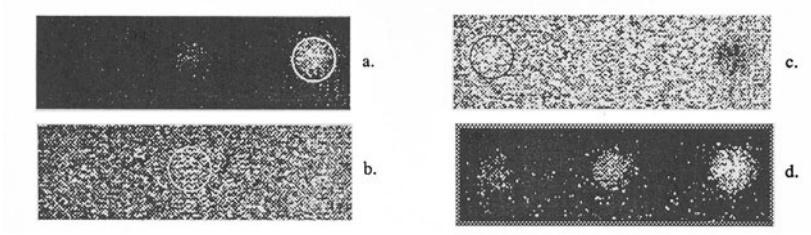

Figure 12. Binned outputs for sample 2 using a corrosion estimator network along with results obtained through a dual network processing -- a. Output of neuron 1 (15%), b. Output of neuron 2 (10%), c. Output of neuron 3 (5%), and d. Dual network results.

used as the input to the network. Beyond 1.6 sec (Frame 7), the data is extremely noisy and the contrast is very poor; consequently, only frames 3-7 were used as the input to the flaw detector network. The thresholded binary image showing all three material loss locations is presented in Fig. 11b. The resulting images obtained through processing the data using an estimator network which was trained using the same 35 training patterns, are presented in Figs. 12 a-c. The flaws are enclosed in circles for reference. The classification is poor in accuracy and the images are extremely noisy. However, a dual network processing gives excellent results as seen in Fig. 12d.

CONCLUSION

A new technique using two neural networks - a flaw detector network and a corrosion estimator network - was used to process thermal data acquired through both quartz lamps heating and flash heating for fabricated corrosion (material loss) samples. The combined result of these two networks which are simple to train, relatively small-sized networks requiring fewer training patterns, is seen to have both high classification and estimation accuracies. Future work will include training networks in the laboratory using simulation and experimental data, and subsequently applying the trained networks to data obtained in the field.

ACKNOWLEDGMENTS

The authors are grateful to Lockheed Corporation for providing fabricated corrosion samples used in this study. They also thank Hazari Syed for his help in providing part of the experimental data. This research was supported under NASA Contract NAS1-19236.

REFERENCES

1. J. S. Heyman, "NDE Research for Aging Aircraft Integrity", *Proceedings of the IEEE 1990 Ultrasonics Symposium*, Honolulu, Hawaii, December 1990.
2. D. R. Prabhu and W. P. Winfree, "Automation of Disbond Detection in Aging Aircraft Through Thermal Image Processing", *Review of Progress in Quantitative Nondestructive Evaluation*, Brunswick, Maine, July 1991.
3. D. R. Prabhu, P. A. Howell, H. I. Syed, and W. P. Winfree, "Application of Artificial Neural Networks to Thermal Detection of Disbonds", *Review of Progress in Quantitative Nondestructive Evaluation*, Brunswick, Maine, July 1991.
4. D. E. Rumelhart, J. L. McClelland, and the PDP Research Group, "Parallel Distributed Processing -- Explorations in the Microstructure of Cognition", The MIT Press, Cambridge, MA, 1986.